The Effect of Hydrogenation on Structure and Superconducting Properties of FeTe0.65Se0.35 Single Crystals

S. I. Bondarenko
B. Verkin Institute for Low Temperature Physics and Engineering, National Academy of Sciences of Ukraine

A. I. Prokhvatilov
B. Verkin Institute for Low Temperature Physics and Engineering, National Academy of Sciences of Ukraine

Roman Puzniak (puzni@ifpan.edu.pl)
Institute of Physics of the Polish Academy of Sciences, Aleja Lotników 32/46, PL-02668 Warsaw, Poland

Jaroslaw Pietosa
Institute of Physics of the Polish Academy of Sciences

A. A. Prokhorov
Institute of Physics of the Czech Academy of Sciences

V. V. Meleshko
B. Verkin Institute for Low Temperature Physics and Engineering, National Academy of Sciences of Ukraine

V. P. Timofeev
B. Verkin Institute for Low Temperature Physics and Engineering, National Academy of Sciences of Ukraine

V. P. Koverya
B. Verkin Institute for Low Temperature Physics and Engineering, National Academy of Sciences of Ukraine

D. J. Gawryluk
Paul Scherrer Institute

Andrzej Wisniewski
Institute of Physics of the Polish Academy of Sciences

Research Article

Keywords: critical temperature, Electron paramagnetic resonance, superconducting state, hydrogenated crystals

Posted Date: March 8th, 2021

DOI: https://doi.org/10.21203/rs.3.rs-267794/v1

The effect of hydrogenation on structure and superconducting properties of $FeTe_{0.65}Se_{0.35}$ single crystals

S. I. Bondarenko[1], A. I. Prokhvatilov[1], R. Puźniak[2, #], J. Piętosa[2], A. A. Prokhorov[3], V. V. Meleshko[1], V. P. Timofeev[1], V. P. Koverya[1], D. J. Gawryluk[2,4], and A .Wiśniewski[2]

[1]B. Verkin Institute for Low Temperature Physics and Engineering, National Academy of Sciences of Ukraine, ave. Nauky 47, 61103 Kharkov, Ukraine
[2]Institute of Physics of the Polish Academy of Sciences, Aleja Lotników 32/46, PL-02668 Warsaw, Poland
[3]Institute of Physics of the Czech Academy of Sciences, Na Slovance, 182 21 Praha 8, Czech Republic
[4]Laboratory for Scientific Developments and Novel Materials, Paul Scherrer Institute, CH-5232 Villigen PSI, Switzerland

[#]E-mail: puzni@ifpan.edu.pl

Abstract

Single crystals of $FeTe_{0.65}Se_{0.35}$, with the onset of critical temperature (T_c) at 14 K, were hydrogenated for 10–90 hours at various temperatures, ranging from 20 to 250 ^oC. It is shown that tetragonal matrix becomes unstable and crystal symmetry is reduced for the crystals hydrogenated already at 200 ^oC despite that molecular impurities do not change matrix symmetry, unless the material is not destroyed under hydrogenation at 250 ^oC. Bulk T_c, taken at the middle of the transition, equal to about 12–13 K for the as-grown $FeTe_{0.65}Se_{0.35}$, increases by 1–2 K. The critical current density determined in magnetic field range of 0–70 kOe increases 4–30 times as a result of hydrogenation at 200 ^oC for 10 h. Electron paramagnetic resonance studies confirmed higher value of the bulk T_c for hydrogenated crystals. Thermal diffusion of hydrogen leads to substantial structural changes, causes degeneration of crystal quality, and significantly affects superconducting properties. A strong correlation was observed between the structural changes and changes in the parameters of the superconducting state for the hydrogenated crystals.

1. Introduction

Over past few years, high values of superconducting transition temperature, close to the room temperatures, have been found mainly in the compounds containing hydrogen subjected to high external pressure.[1-5] On the other hand, at ambient pressure, for a number of compounds, including metallic, cuprate, pnictide, and carbon-based materials, an impact of hydrogen causes a noticeable improvement in their superconducting properties.[6] Particularly in BCS superconductors, hydrogen introduces new phonon modes, what strongly affects superconducting properties due to anharmonicity of hydrogen related vibrations. Additionally, hydrogen is a very useful tool in testing mechanisms of superconductivity due to the availability of the deuterium – isotope with double atomic mass.

It was found that hydrogenation is an efficient tool for increasing flux pining properties of superconductors. For example, it was shown that lattice defects, including dislocations, grain boundaries and impurities such as hydrogen that generate hydride precipitates, effectively suppress the expulsion of magnetic field and pin the field inside the material even after the external magnetic field is removed.[7,8] The effect of hydrogenation on properties of highly textured $YBa_2Cu_3O_y$ ceramics was studied by Bobylev *et al.*[9] It was shown that the critical current density and first critical field, in the samples with high oxygen contents (y = 6.96) hydrogenated at T = 150 °C and subsequently oxygenated, increase in comparison to that in the initial state. According to the authors, partial reduction of copper with formation of microinclusions of Cu_2O and other products of chemical decomposition, which are extra pinning centers of magnetic vortices, occurs after hydrogenation.

For iron-based superconductors it was noticed that hydrogen plays important role both in the synthesis process and in modification of superconducting properties, especially increasing T_c in some compounds.[10] Nakamura and Machida[11] have tried to explain the origin of T_c enhancement due to hydrogen doping using first-principles calculations. They concluded that the most stable location of hydrogen atoms in 1111-type $LaFeAsOH_x$ superconductors is near Fe sites and that makes the crystal structure more suitable for superconductivity.

It was shown that for niobium chalcogenides, quasi-two-dimensional crystalline structure of these compounds is very sensitive to the presence of non-magnetic atomic and molecular impurities (hydrogen, air components, *etc.*).[12,13]

It is well established now that the incorporation of hydrogen into iron chalcogenide superconductors (ICS), applying various methods, changes their superconducting state properties. The bombardment of FeSe with hydrogen ions leads to an increase in the

sharpness of superconducting transition.[14] The electrochemical introduction of hydrogen ions caused enhancement of superconducting transition temperature T_c from 6 to 43.5 K for $FeSe_{0.93}S_{0.07}$ and from 8.5 to 41 K for FeSe.[15] Annealing of the Fe-Te-Se compound in an oxygen atmosphere at temperatures of 300–400 °C leads to a strong changes in superconducting properties[16] and subsequent annealing of this compound in hydrogen causes an increase in the steepness of the superconducting transition.[17] Finally, the chemical combination of FeSe with tetrabutyl ammonium (TBA), each molecule of which contains 36 hydrogen atoms, shifted a critical temperature in $(TBA)_{0.3}FeSe$ to the level of 50 K (from T_c = 8 K for FeSe), what is currently record-breaking for bulk single crystals of this family of ICSs.[18]

Recently performed x-ray structural studies of Fe-Te-Se showed[19] that air molecules change the interlayer interaction in the tetragonal phase of the Fe-Te-Se and come up with a significant effect on the structural parameters of this superconductor. Pronounced structural changes occur under the influence of diffuse penetration of hot hydrogen (at the temperature of about 200 ^oC) into the sample. At this temperature, a structural phase transition of the tetragonal lattice to the orthorhombic one is observed. Moreover, the interaction of hydrogen with the matrix is changed at transition temperature, i.e., the van der Waals interaction in the tetragonal structure is changed to the chemical one in the orthorhombic phase. The latter becomes possible due to the thermocatalytic dissociation of molecular hydrogen in the $FeTe_{0.65}Se_{0.35}$–H_2 system.[20] It should be noted that the phase transition is observed only due to the impact of hydrogen atoms.

In this paper, correlation between structural changes and superconducting properties observed for hydrogenated $FeTe_{0.65}Se_{0.35}$ single crystals was studied. Observed very significant increase in the critical current density is explained by the appearance of additional pinning centers due to significant mechanical stresses associated with the rearrangement of the crystal lattice after hydrogenation.

2. Experimental details

The studied crystals of $FeTe_{0.65}Se_{0.35}$, usually in the form of well-developed plates, with a tetragonal lattice of *P*4/*nmm* symmetry at room temperature and with the crystal lattice parameters: $a = b = 3.799$ Å, $c = 6.093$ Å, $V = 87.9$ Å^3,[21,22] were grown from a melt by the Bridgman method. The samples were prepared from stoichiometric quantities of Fe chips (3N5), tellurium powder (4N) and high purity Se powder (5N). All of the materials were

weighed and mixed in an argon filled glove box. Double walled evacuated (9×10^{-5} Pa) and sealed quartz ampoules with starting materials were placed in a furnace with an average vertical gradient of temperature equal to ~ 1.0 °C mm^{-1}. The material was synthesized for 6 h at temperature up to 700 °C. After melting at ~ 860–880 °C the temperature was held for 3 h and then was reduced down at a rate of 1 °C h^{-1} and thus, the growth velocities of the crystals were equal to ~ 1 mm h^{-1}.

Structural studies were carried out with polycrystalline x-ray diffractometer using radiation of Cu-K_α copper anode with $\lambda = 1.54178$ Å. The beta radiation of the x-ray tube was significantly attenuated using the appropriate Ni filter. The diffraction data were obtained from close-packed basal planes (00l).

After growing the crystals were maintained in the air atmosphere for several weeks. In order to remove air components captured during growth and after the process, as well as, to reduce the level of internal stresses, the samples were evacuated for up to 200 hours at pressures of about 0.13 Pa in stainless steel chamber. Next, the crystals were removed from the chamber and they were mechanically cleaved along one of the (00l) planes which are tightly packed and loosely connected by the van der Waals forces. An analysis of x-ray diffraction patterns taken from fresh cleaved crystal yielded data for a pure crystal. At the next stage, all of the studied samples were subjected to prolonged exposure to hydrogen at various temperatures for the time sufficiently long to reach hydrogen saturation. The samples were hydrogenated during 10–90 hours (shorter time for higher temperatures) at the temperatures of 20, 100, 150, 180, 200, 250 °C at a hydrogen gas pressure of 5×10^5 Pa and structural measurements were repeated.

Magnetic characteristics were studied in the temperature range from 2 to 300 K, in magnetic fields up to 70 kOe, with MPMS-**7** SQUID magnetometer, and the dependences of magnetic moment on temperature and magnetic field were recorded. Superconducting transition temperature was determined from zero-field cooling $M(T)$ measurements. The critical current densities were evaluated from hysteresis loops recorded at fixed temperature, using the Bean model. The isothermal relaxation of the residual magnetization of the crystal, $M(t)$, was recorded as well.

Continuous wave EPR spectra were recorded using a Brucker X-/Q-band E580 FT/CW ELEXSYS spectrometer within the temperature range of 4–18 K. For the measurements, the ER 4122 SHQE Super X High-Q cavity with TE011 mode was used. The samples were placed into quartz rods of 4 mm in diameter. The experimental parameters

were: micro-wave frequency 9.407 GHz, microwave power 0.1500 mW, modulation frequency 100 kHz, modulation amplitude 0.2 mT, and the conversion time of 60 ms.

3. Results and discussion

3.1 Structural properties

Analyzing the obtained diffraction patterns, special attention was paid to the effect of hydrogen on the intensity, half-width, and structure of studied crystals. It was found that in the studied temperature range of hydrogenation: 20–250 °C, with increasing temperature, the mechanisms of hydrogen sorption and crystal symmetry change (see, Fig. 1). The tetragonal phase with the van der Waals interaction of hydrogen molecules with matrix is stable at low temperatures. Under the influence of the catalytic effect of Fe atoms in $FeTe_{0.65}Se_{0.35}+H_2$ solutions at a temperature of about 200 ^oC, hydrogen molecules (possibly also impurity oxygen molecules at lower temperatures) dissociate. This process is accompanied by a sharp increase in the concentration of molecular ions, an increase in the magnitude of stresses, as well as the heterogeneity of local strains of interatomic chemical bonds (Fig. 1). Due to the large difference in the diameters of interacting particles in the resulting substitution solutions, an increase in the level of local displacement defects and internal stresses is observed with an increase in the concentration of hydrogen molecules. At certain temperatures and external pressures, the internal chemical pressure reaches a critical value. As a result of the combination of these factors, the tetragonal lattice of iron chalcogenide loses stability, which entails a structural phase transition at which the relaxation of internal local stresses occurs, and the crystal symmetry decreases to orthorhombic one. From Fig. 1b it follows that the phase transition occurs near a temperature of 200 °C, where the form of diffraction patterns changes. In the temperature range of 20–180 °C, x-ray diffraction patterns of $FeTe_{0.65}Se_{0.35}$ single crystal, incubated for 10 hours in hydrogen under an external pressure of gaseous hydrogen of 5×10^5 Pa contain only reflections (00l) from the basal planes of the tetragonal lattice (Fig. 1a). With their further heating near 200 °C, an additional doublet of (010) (100) reflections of the orthorhombic lattice arises (Fig. 1c). An abnormal change in the intensity and half-width of the lines of diffraction reflections also occurs in the region of structural phase transition (Fig. 1b).

The data in Fig. 1 indicate that in the studied crystals with an atomic impurity of H^+, the relaxation of stresses and local deformations near defects occurs at the phase transition

from the tetragonal to the orthorhombic symmetry. The transition is accompanied by strong lattice compression at which the crystal density increases by almost 15%.[19]

3.2. Superconducting properties

Figure 2a shows temperature dependence of dc magnetic susceptibility $\chi(T)$ of the studied crystals in the region of the superconducting phase transition. The $\chi(T)$ curves are shown both for pristine sample and after hydrogenation at temperatures of 180, 200, and 250 °C for 10 hours. One can see that the bulk critical temperature (T_c^{bulk}) increases by approximately 2 K after hydrogenation at 180 and 200 °C. After treatment with hydrogen at temperature of 250 °C, the critical temperature of the sample decreases to about 9 K. Comparison of the structural data (Fig. 1) and observed tendency in the critical temperature shows that increase in T_c^{bulk} observed after hydrogenation at 180 and 200 °C apparently correlates with an increase of the intensity, width, and angular position of the (001) diffraction peak.

An important characteristic of a superconductor, which determines its magnetic and current-carrying capabilities, is the ability to pin vortices trapped in the volume . To study the dynamics of magnetic flux in $FeTe_{0.65}Se_{0.35}$, the measurements were carried out in the field cooling mode (FC). When the magnetic field is turned off, the residual magnetization of the sample and its dynamic are determined by the state of the captured magnetic flux in the bulk of the superconductor. The role of near-surface energy barriers (for example, the Bean-Levingston barrier), which are difficult to control and analyze, in the dynamic of magnetic flux under these conditions is minimal.

The thermally activated creep of individual vortices and their bundles can lead to the redistribution and weakening of bulk superconducting currents. In this case, the integral magnetic moment $m(t)$ may decrease. As a result, the averaged magnetization M of the superconducting sample can relax in time.[22] In contrast to this expected behavior, we found that after the hydrogenation at temperatures of 180–250 °C, relaxation was practically absent (Fig. 2b). This indicates that this treatment forms new and very powerful vortex pinning centers in the crystal.

In the case of the $FeTe_{0.65}Se_{0.35}$ crystal, one should take into account the presence of excess Fe, as well as magnetic inclusions such as Fe_3O_4 and Fe_7Se_8, which are located in the interlayer space of the superconductor and on its surface.[22-24] As a result, the magnetization of sample, M, is a superposition of two contributions $M \approx M_F + M_D$, where M_F and M_D are the

ferromagnetic and diamagnetic contributions, respectively. As a result, the magnetization loop $M(H)$ becomes asymmetric (Fig. 3a) with respect to the H-axis, which indicates the possible influence of the Bean-Levingston surface barrier, the presence of an uncompensated magnetic moment of Fe ions, as well as other Fe-based inclusions.[21-24]

The impact of an uncompensated magnetic moment of Fe ions and/or other Fe-based inclusions on the shape of hysteresis loop in the studied materials seems to be dominant. The asymmetry of the loop for the sample hydrogenated at 250 ^{o}C is significantly reduced as compared to that one for the as-grown sample and for the samples hydrogenated at 180 and 200 ^{o}C. However, the shape of reversible contribution to hysteresis loop, recorded in quite wide temperature range from 5 to 12 K for the sample hydrogenated at 200 ^{o}C (see, Fig. 3c), remaining practically unchanged despite significant changes of superconducting state properties, indicate on its magnetic origin.

According to the Bean critical state model, the critical current density j_c can be estimated using the well-known formula $j_c = 20\Delta M/[a(1-a/3b)]$, where a, b ($a < b$) are the sizes of the cross section of the sample and ΔM is the width of the $M(H)$ loop.[25]

As one can see in Fig. 3a, the width of the hysteresis loop, ΔM, is significantly larger for hydrogenated crystal as compared with the pristine one and only slightly decreases with increasing field up to 70 kOe. Apparently, the defects generated in the structure during hydrogenation are very effective pinning centers. The largest ΔM is observed for the crystal hydrogenated at 200 ^{o}C. This correlates well with the observed structural rearrangement observed for $FeTe_{0.65}Se_{0.35}$ crystal due to hydrogenation. As it was shown above, at 200° C the structural phase transition of the tetragonal lattice to the orthorhombic one is observed. On the other hand, the hydrogenation at 250 °C leads to amorphization of $FeTe_{0.65}Se_{0.35}$ compound[19] In consequence, superconducting properties: critical temperature as well as capability to carry the superconducting current are much poorer. It can be assumed that its diamagnetic properties will be violated. Measurements of the $M(H)$ dependence for the sample processed at temperature of 250 °C completely confirmed this assumption. The diamagnetic magnetization of the crystal significantly decreases even in relatively weak fields (less than 100 Oe), and at large values it disappears altogether (Fig. 3a).

Figure 3b shows the values of the critical current density of the crystals before and after their treatment with hydrogen, based on the $M(H)$ dependences presented in Fig. 3a. The width of the hysteresis loop for a single crystal before hydrogenation, presented in Fig. 3a, is never larger than that for the crystal hydrogenated at 180 ^{o}C. However, the j_c values for

pristine crystal at low fields are slightly larger than those for the crystal hydrogenated at 180 °C because of some differences in the size of studied crystals, affecting the width of measured hysteresis loop.

It can be apparently seen that treatment with hydrogen increases the value of j_c. The highest values of j_c, are observed for the crystal hydrogenated at 200 °C. Especially spectacular is increase of j_c at higher magnetic fields. In fact, for fields higher than 5 kOe the $j_c(H)$ dependence is almost flat, both for the crystal hydrogenated at 180 and 200 °C. For the crystal hydrogenated at 200 °C, at high magnetic fields, the j_c is at a level of 3×10^3 A/cm^2). This shows that introduced pinning centers are very robust and effective in high magnetic fields.

The critical current density of about 4 times greater in the fields up to 20 kOe at a temperature of 7 K then that for pristine crystal, were achieved in the crystal treated with hydrogen at temperature of 200 °C. This difference increases in the fields higher than 20 kOe, and in the field of 70 kOe ratio of both critical current densities reaches the value of about 30 (see, Fig. 3b). It should also be noted that in the range of fields of 10–70 kOe, the j_c of such a crystal practically does not change. The maximum value of j_c in the zero field at temperature of 7 K is 10^4 A/cm^2. Somehow unexpected is the same high critical current density in a zero field in a crystal treated at a hydrogen temperature of 250 ° C, although the superconductivity in it is destroyed even in a weak magnetic field.

Evolution of $j_c(H)$ with temperature for the sample hydrogenated at 200 °C is presented in Fig. 3d. Obtained data show high j_c values for the fields below 60 kOe and temperatures below 9 K.

Since the volume of the crystal lattice decreases by about 15% after hydrogenation,[19] this leads to large chemical pressure effect. Hence, observed increase in the critical current density can be explained by the appearance of additional pinning centers due to significant mechanical stresses associated with the rearrangement of the crystal lattice after hydrogenation.

3.3. EPR studies

Since the most pronounced improvement of superconducting properties was observed for the crystal hydrogenated at 200 °C, the EPR studies were performed for the pristine (not hydrogenated) crystal and for the crystal hydrogenated at 200 °C.

Absorption line in the zero field is clearly seen for both studied crystals. However, substantial difference between the samples is observed in the form of an EPR line at a superconducting transition. For the as-grown crystal, a significant change in the absorption line occurs in the temperature range T = 10–13 K, which corresponds to phase transitions in the material (see, Fig. 4a). For the crystal hydrogenated at 200 ^{o}C, a wide asymmetric line is observed in the temperature range of 4–18 K, which changes significantly with decreasing temperature from 14 to 12 K, which can be characterized as a result of the phase transition (see, Fig. 4b). It means that transition to superconducting state for the sample hydrogenated at 200 ^{o}C is located in higher temperature range than that one for the as-grown sample. At temperatures above T_c, the dependence of the EPR line on temperature is not observed. Temperature dependence of the integrated intensity of the absorption line in the region close to bulk superconducting transition at about 13 K for both: as-grown and hydrogenated at 200 ^{o}C single crystals is presented in Fig. 4c.

4. Conclusions

It was shown that hydrogenation strongly affects structural and superconducting properties of $FeTe_{0.65}Se_{0.35}$ single crystals. When performed at too high temperatures (250 ^{o}C in the case of current studies) it leads to amorphization of the crystal and to strong degradation of its superconducting properties. On the other hand, hydrogenation performed at temperature 180–200 ^{o}C strongly improves superconducting properties. Bulk critical temperature increases by 1–2 K and transition to superconducting state becomes sharper. The new, very effective pinning centers are introduced what is manifested by strong increase in the value of the critical current density (4-30 times), as compared with pristine sample. After hydrogenation also relaxation of magnetization is practically absent. The hydrogenation causes pronounced changes in the crystallographic structure. Structural transition from tetragonal to orthorhombic structure occurs during hydrogen treatment at temperature of 180–200 °C. Obtained results confirm that the inhomogeneous spatial distribution of ions in chalcogenides with nanoscale phase separation enhances the superconductivity in this system. The conclusions drawn here from the magnetic measurements are in line with those drawn from the transport measurements performed already on iron-based chalcogenide crystals of various crystallographic quality.[22] However, the improvement of superconducting properties at ambient pressure, reported here, was obtained as a result of degeneration of crystallographic quality in hydrogenation process for a specific crystal. Importantly, it was not

a result of tailoring crystal growth conditions, leading to the growth of crystals with distinct crystallographic quality and thus with distinct superconducting properties. EPR studies confirmed shift of bulk superconducting transition to higher temperature range as a result of hydrogenation.

Acknowledgements

This work was partially supported by the National Science Centre of Poland based on decision No. DEC-2013/08/M/ST3/00927. The authors thank Kh. B. Chashka for a useful discussion of the results presented in current manuscript. The EPR measurements were carried out within infrastructure SAFMAT in FZU CAS. This research was supported by the Czech Science Foundation (GACR), Project No. 19-16315S. We acknowledge the Operational Program Research, Development and Education financed by European Structural and Investment Funds and the Czech Ministry of Education, Youth and Sports (Projects SAFMAT - CZ.02.1.01/0.0/0.0/16_013/0001406 and SOLID21 CZ.02.1.01/0.0/0.0/16_019/0000760).

Data availability

The data that support the findings of this study are available from the corresponding author upon reasonable request.

References

1. Eremets, M. I. & Drozdov, A. P. High-temperature conventional superconductivity. *Physics-Uspekhi* **59**, 1154-1160 (2016).
2. Gor'kov, L. P. & Kresin, V. Z. High pressure and road to room temperature superconductivity. *Rev. Mod. Phys.* **90**, 011001 (2018).
3. Drozdov, A. P., Eremets, M. I., Trojan, I. A., Ksenofontov, V. & Shylin, S. I. Conventional superconductivity at 203 Kelvin at high pressure in the sulfur hydride system. *Nature* **525**, 73-76 (2015).
4. Somayazulu, M. *et al*. Evidence for superconductivity above 260 K in lantanum superhydride at megabar pressure. *Phys. Rev. Lett.* **122**, 027001 (2019).

5. Liu, H., Naumov, I. I., Hoffmann, R., Ashcroft, N. W. & Hemley, R. J. Potential high-T_c superconducting lanthanum and yttrium hydrides at high pressure. *PNAS of the USA* **114**, 6990-6995 (2017).

6. Syed, H. M., Webb, C. J., Gray, E. M. Hydrogen-modified superconductors: A review. *Progress in Solid State Chemistry* **44**, 20-34 (2016).

7. Knobloch, J. & Padamsee, H. Flux trapping in niobium cavities during breakdown events. *Proceedings of the 1997 Workshop on RF Superconductivity, Abano Terme, Padova* (INFN, Italy, 1997) 337-344 (1997).

8. Vallet, C. *et al*. Flux trapping in superconducting cavities. *Proceedings of the Third European Particle Accelerator Conference* (Frontières, Gif-sur-Yvette, 1992) **2**, 1295-1297 (1992).

9. Bobylev, I. B., Gerasimova, E. G, Zyuzeva, N. A., Terent'ev, P. B. Effect of hydrogen intercalation on the critical parameters of $YBa_2Cu_3O_y$. *Physics of Metals and Metallography* **118**, 954-964 (2017).

10. Hanna, T. *el al*. Hydrogen in layered iron arsenides: indirect electron doping to induce superconductivity. *Phys. Rev. B* **84**, 024521 (2011).

11. Nakamura, H. & Machida, M. First-principles studies for the hydrogen doping effects on iron-based superconductors. *J Phys. Soc. Jpn*. **80**, 073705 (2011).

12. Obolenskii, M. A., Beletskii, V. I., Chashka, K. B., & Basteev, A. V. Enhancement of the superconducting state in the 2H-$NbSe_2$ hydrogen system. *Soviet Journal of Low Temperature Physics* **10**, 402-403 (1984).

13. Chashka, Kh. B., Obolensky, M. A., Beletsky, V. I., & Beilinson, V. N. Heat capacity of the $NbSe_2$-hydrogen system. *Low Temp. Phys.* **12**, 865-869 (1986).

14. Burkhanov, G. S. *et al*. Hydrogen intercalation of compounds with FeSe and $MoSe_2$ layered crystal structures. *Inorganic Materials: Appl. Res.* **8**, 759-762 (2017).

15. Cui, Yi. *et al.* Ionic-liquid-gating induced protonation and superconductivity in FeSe, $FeSe_{0.93}S_{0.07}$, ZrNCl, 1T-TaS_2 and Bi_2Se_3. *China Phys. Lett.* **36**, 077401 (2019).

16. Sun, Y., Shi, Z. & Tamagai, T. Review of annealing effects and superconductivity in $Fe_{1-y}Te_{1-x}Se$ superconductors. *Supercond. Sci. Technol.* **32**, 103001 (2019).

17. Friederichs, G. M., Worsching, M. P. B. & Johrendt, D. Oxygen-annealing effects on superconductivity in polycrystalline $Fe_{1+x}Te_{1-y}Se_y$. *Supercond. Sci. Technol.* **28**, 095005 (2015).

18. Shi, M. Z. *et al*. FeSe–based superconductors with a superconducting transition temperature of 50 K. *New J. Phys.* **20**, 123007 (2018).
19. Prokhvatilov, A. I., Meleshko, V. V., Bondarenko, S. I., Koverya, V. P. & Wiśniewski, A. The effect of sorption of air and hydrogen components on the structural characteristics of superconducting single crystals $FeTe_{0.65}Se_{0.35}$. *Low Temp. Phys.* **46**, 181-186 (2020).
20. Yagotintsev, K. A. *et al*. Saturation of C60 fullerite with hydrogen: study of the adsorption crossover. *Low Temp. Phys.* **38**, 952-956 (2012).
21. Bao, W. *et al.* Tunable ($\delta\pi$, $\delta\pi$)-type antiferromagnetic order in α-Fe(Te,Se) superconductors. *Phys. Rev. Lett.* **102**, 247001 (2009).
22. Tsurkan, V. *et al*. Physical properties of $FeSe_{0.5}Te_{0.5}$ single crystals grown under different conditions. *Eur. Phys. J. B* **79**, 289-299 (2011).
23. Sivakov, A. G. *et al.* Microstructural and transport properties of superconducting $FeTe_{0.65}Se_{0.35}$ crystals. *Supercond. Sci. Technol.* **30**, 015018 (2017).
24. Galluzzi, A. *et al*. Mixed state properties of iron based Fe(Se,Te) superconductor fabricated by Bridgman and by self-flux methods. *J. Appl. Phys.* **123**, 233904 (2018).
25. Wiesinger, H. P., Sauerzopf, F.M. & Weber, H. W. On the calculation of J_c from magnetization measurements on superconductors. *Physica C* **203**, 121-128 (1992).

Figure captions

Figure 1. (a) X-ray diffraction patterns for $FeTe_{0.65}Se_{0.35}$ crystals obtained for initial state after prolonged exposure to air and after exposing the crystal to hydrogen at a pressure of 5×10^5 Pa at temperature of 20 ^oC for 90 h; at 180 ^oC for 10 h; at 200 ^oC for 10 h; at 250 ^oC for 10 h. All of the diffractograms have been shifted vertically, by 5×10^3 between each pattern, for clarity. (b) Changes in the structural characteristics of the first diffraction line (001) after the hydrogenation: (1) - initial state after prolonged exposure to air; (2) - after exposing the crystal to hydrogen at a pressure of 5×10^5 Pa at temperature of 20 ^oC for 90 h; (3) - exposing at 100 ^oC for 10 h; (4) - exposing at 150 ^oC for 10 h; (5) - exposing at 180 ^oC for 10 h; (6) - exposing at 200 ^oC for 10 h; (7) - exposing at 250 ^oC for 10 h. (c) Formation of a qualitatively new diffraction pattern, displaying a rather intense asymmetric maximum at reflection angles $2\Theta \sim 24–26^o$ appearing after exposing the crystal to hydrogen at temperature of 200 ^oC. Black line is a sum of red (peak 010) and blue (peak 100) lines.

Figure 2. (a) Temperature dependence of dc magnetic susceptibility, recorded in zero field cooling mode in H = 10 Oe parallel to the c-axis, for the as-grown single crystal of $FeTe_{0.65}Se_{0.35}$ and after hydrogenation at 180, 200, and 250 °C. (b) Time dependence of the magnetization, $M(t)$, normalized to its maximum initial value, M_0, measured at 5 K after field cooling in magnetic field of 5 Oe, parallel to the c-axis, for the crystals hydrogenated at 180, 200, and 250 ^oC.

Figure 3. (a) Magnetization hysteresis loops recorded at 7 K for pristine $FeTe_{0.65}Se_{0.35}$ crystal and for the crystals hydrogenated at 180, 200, and 250 ^oC. (b) Field dependence of critical current density, j_c, at 7 K for $FeTe_{0.65}Se_{0.35}$ single crystal: pristine and hydrogenated at 180, 200, and 250 ^oC. (c) Hysteresis loops recorded in the temperature range from 5 to 12 K for the crystal hydrogenated at 200 ^oC. (d) Comparison of field dependence of j_c, recorded at various temperatures in the temperature range from 5 to 12 K, for the crystal hydrogenated at 200 ^oC.

Figure 4. (a, b) Wide asymmetric lines observed in the temperature range of 4–18 K, which change significantly with decreasing temperature from 13 to 10 K (a), and from 14 to 12 K for the crystal hydrogenated at 200 ^oC (b). (c) Temperature dependence of the integrated intensity of the absorption line in the region close to bulk superconducting transition at about 13 K for both: as-grown and hydrogenated at 200 ^oC single crystals of $FeTe_{0.65}Se_{0.35}$.

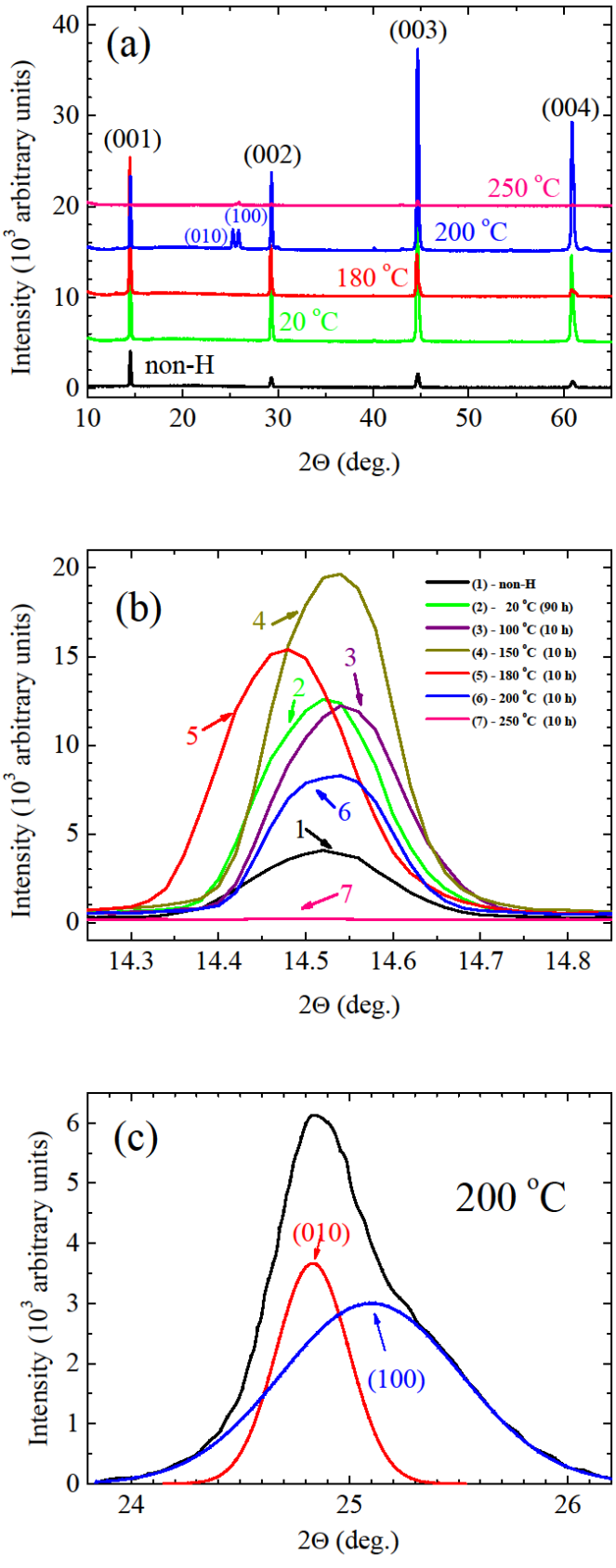
(a)
(001)
(002)
(003)
(004)
(100)
(010)
250 °C
200 °C
180 °C
20 °C
non-H
Intensity (10^3 arbitrary units)
2Θ (deg.)
(b)
(1) - non-H
(2) - 20 °C (90 h)
(3) - 100 °C (10 h)
(4) - 150 °C (10 h)
(5) - 180 °C (10 h)
(6) - 200 °C (10 h)
(7) - 250 °C (10 h)
1
2
3
4
5
6
7
Intensity (10^3 arbitrary units)
2Θ (deg.)
(c)
200 °C
(010)
(100)
Intensity (10^3 arbitrary units)
2Θ (deg.)

Figure 1

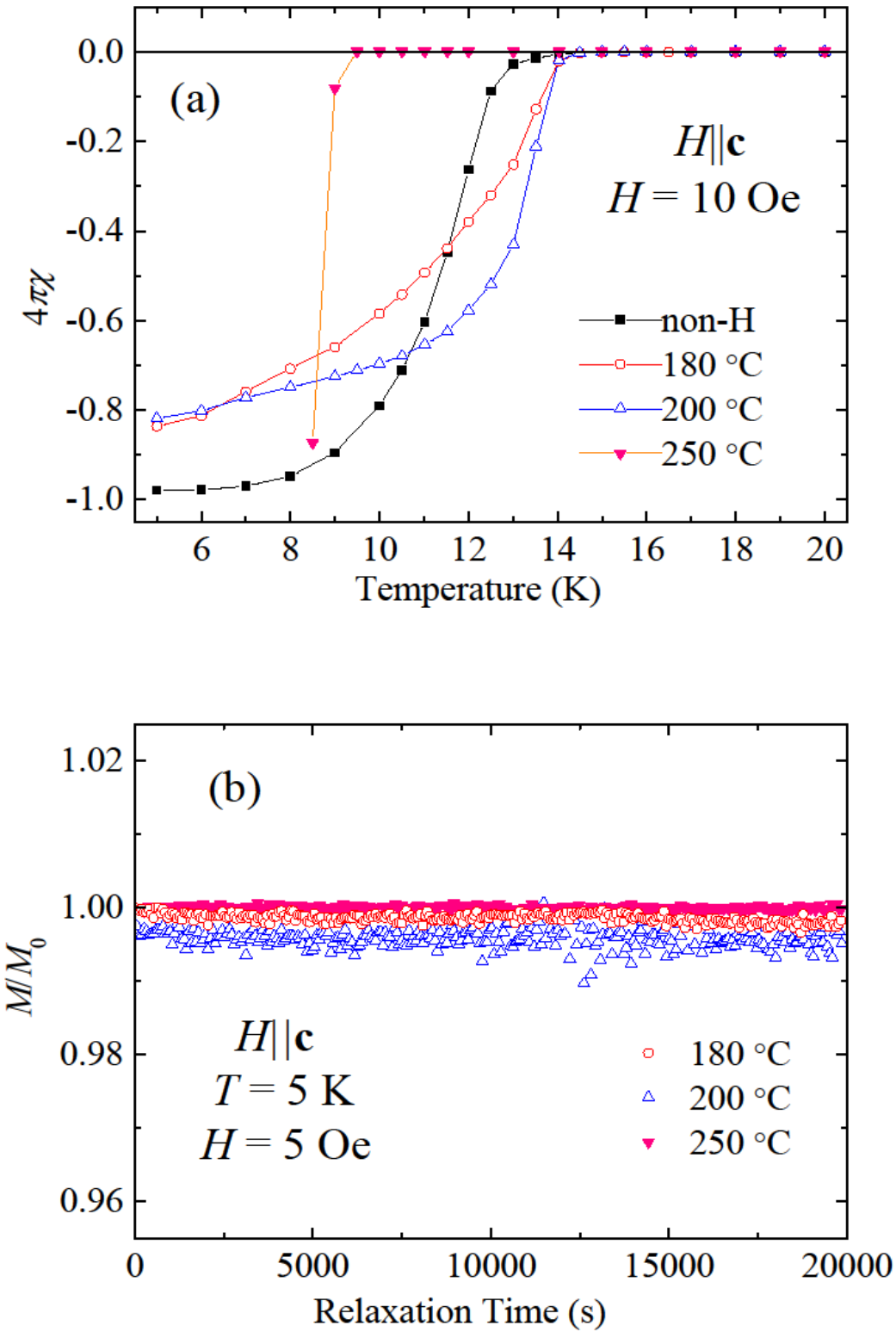
(a)
H||c
H = 10 Oe
non-H
180 °C
200 °C
250 °C
4πχ
Temperature (K)
(b)
H||c
T = 5 K
H = 5 Oe
180 °C
200 °C
250 °C
M/M0
Relaxation Time (s)

Figure 2

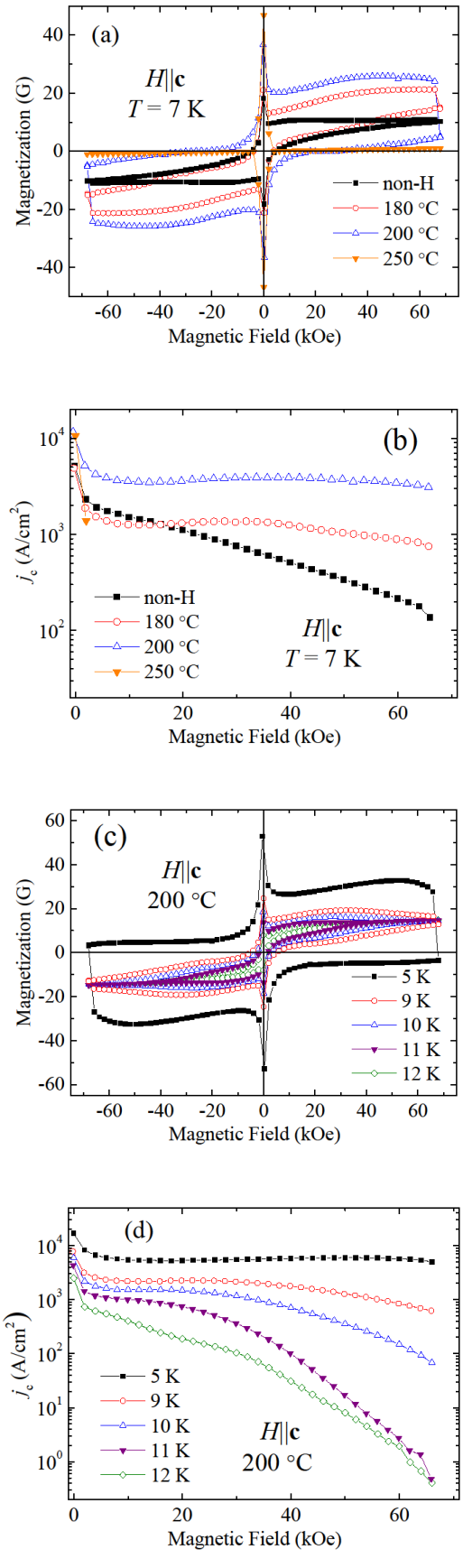
(a)
H||c
T = 7 K
non-H
180 °C
200 °C
250 °C
Magnetization (G)
Magnetic Field (kOe)
(b)
non-H
180 °C
200 °C
250 °C
H||c
T = 7 K
j_c (A/cm^2)
Magnetic Field (kOe)
(c)
H||c
200 °C
5 K
9 K
10 K
11 K
12 K
Magnetization (G)
Magnetic Field (kOe)
(d)
5 K
9 K
10 K
11 K
12 K
H||c
200 °C
j_c (A/cm^2)
Magnetic Field (kOe)

Figure 3

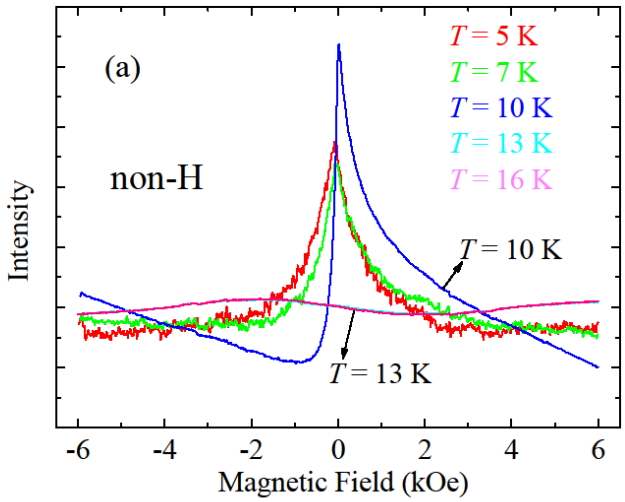
(a)
non-H
T = 5 K
T = 7 K
T = 10 K
T = 13 K
T = 16 K
T = 10 K
T = 13 K
Intensity
-6
-4
-2
0
2
4
6
Magnetic Field (kOe)

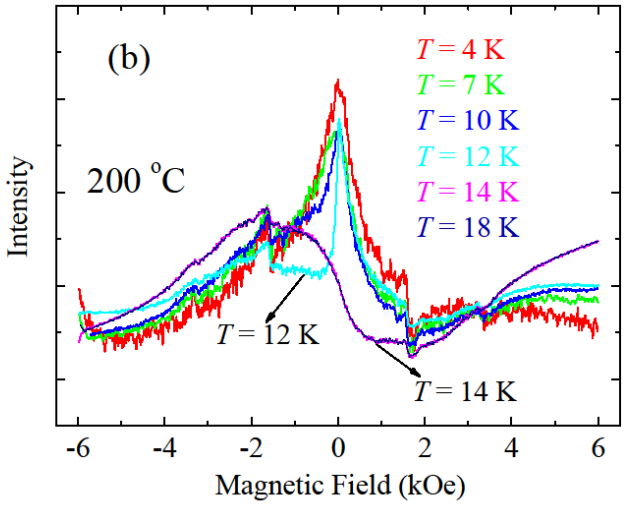
(b)
200 °C
T = 4 K
T = 7 K
T = 10 K
T = 12 K
T = 14 K
T = 18 K
T = 12 K
T = 14 K
Intensity
-6
-4
-2
0
2
4
6
Magnetic Field (kOe)

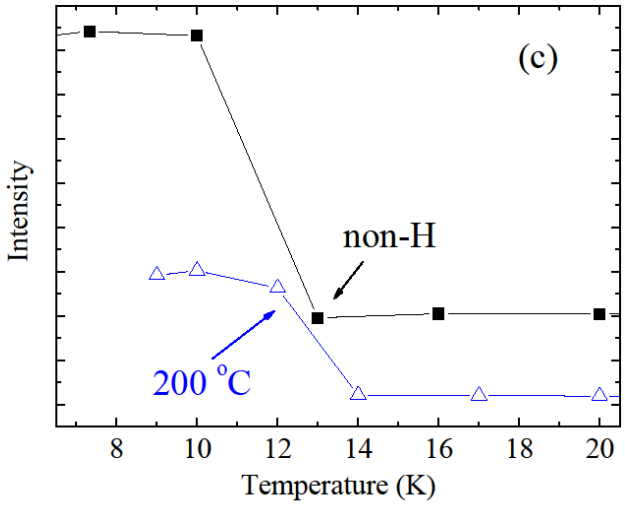
(c)
non-H
200 °C
Intensity
8
10
12
14
16
18
20
Temperature (K)

Figure 4

Figures

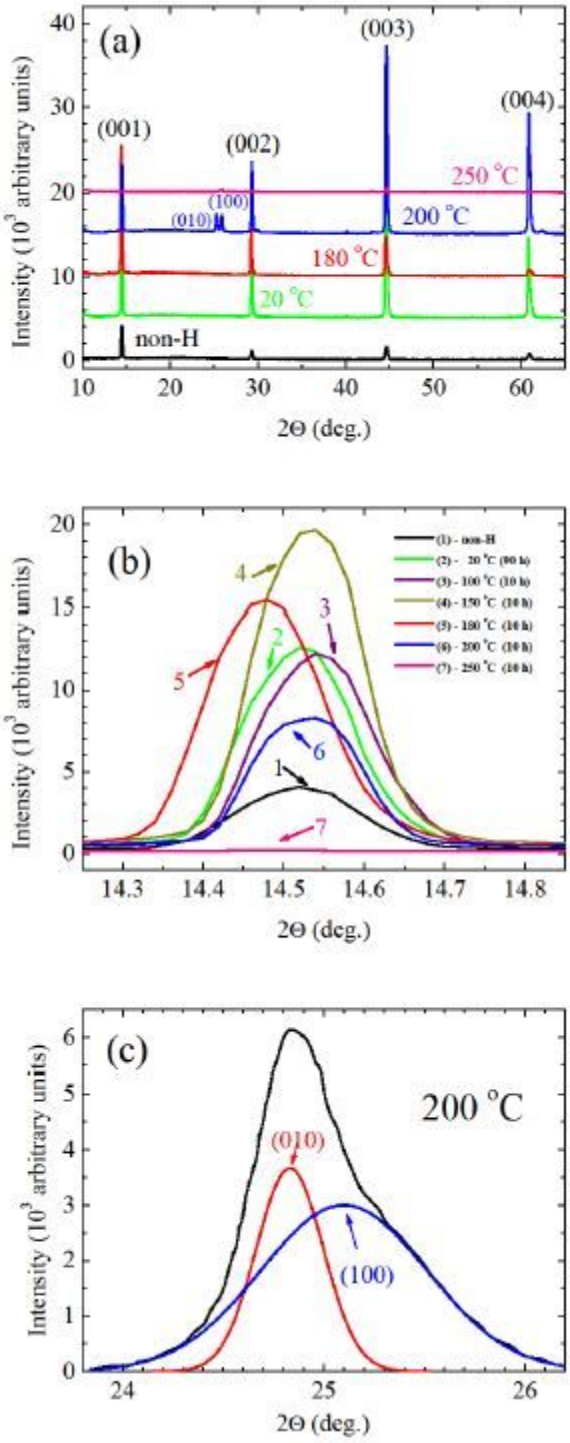

Figure 1

(a) X-ray diffraction patterns for FeTe0.65Se0.35 crystals obtained for initial state after prolonged exposure to air and after exposing the crystal to hydrogen at a pressure of 5×105 Pa at temperature of 20 oC for 90 h; at 180 oC for 10 h; at 200 oC for 10 h; at 250 oC for 10 h. All of the diffractograms have been

shifted vertically, by 5×103 between each pattern, for clarity. (b) Changes in the structural characteristics of the first diffraction line (001) after the hydrogenation: (1) - initial state after prolonged exposure to air; (2) - after exposing the crystal to hydrogen at a pressure of 5×105 Pa at temperature of 20 oC for 90 h; (3) - exposing at 100 oC for 10 h; (4) - exposing at 150 oC for 10 h; (5) - exposing at 180 oC for 10 h; (6) - exposing at 200 oC for 10 h; (7) - exposing at 250 oC for 10 h. (c) Formation of a qualitatively new diffraction pattern, displaying a rather intense asymmetric maximum at reflection angles 2Θ ~ 24–26o appearing after exposing the crystal to hydrogen at temperature of 200 oC. Black line is a sum of red (peak 010) and blue (peak 100) lines.

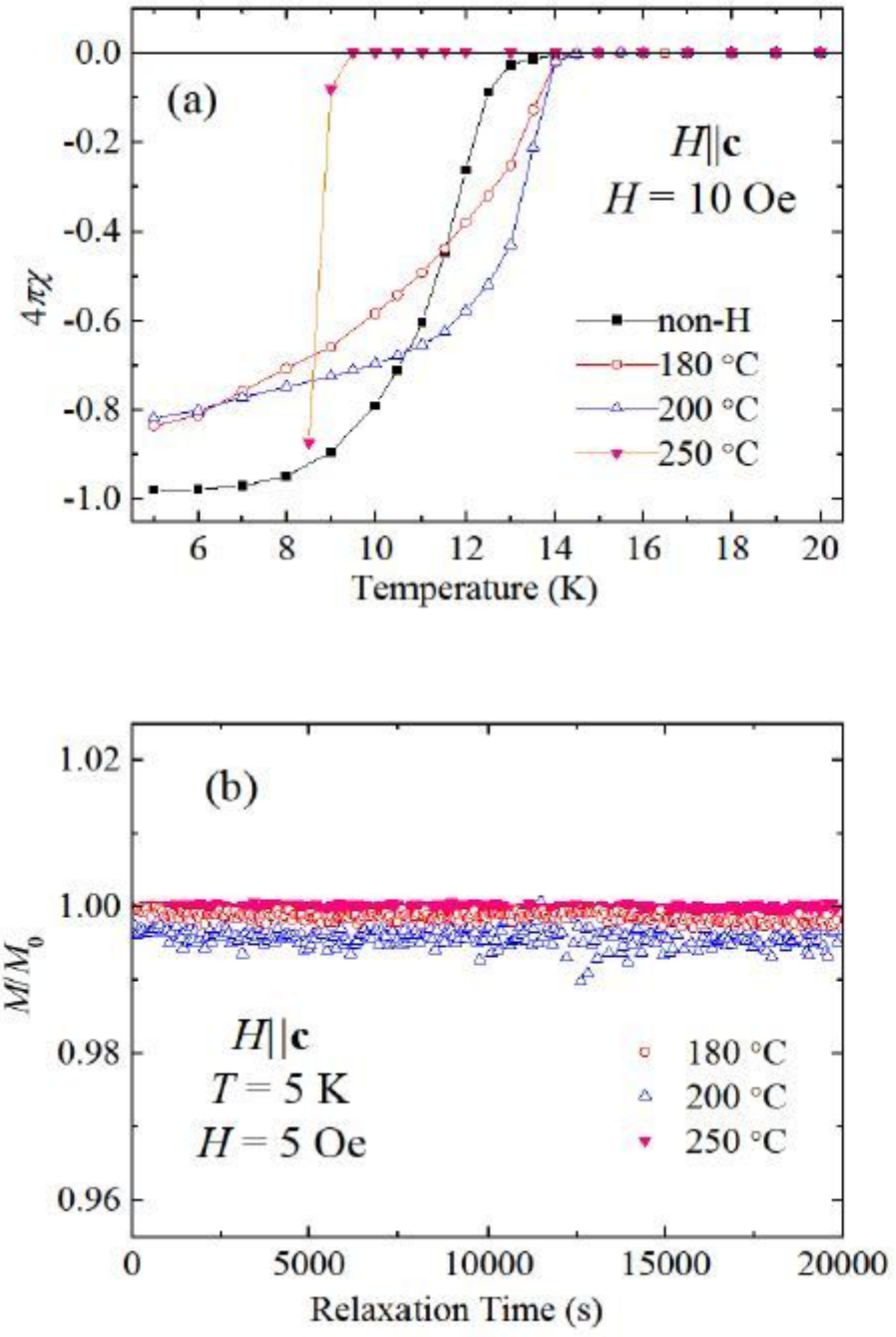

Figure 2

(a) Temperature dependence of dc magnetic susceptibility, recorded in zero field cooling mode in H = 10 Oe parallel to the c-axis, for the as-grown single crystal of FeTe0.65Se0.35 and after hydrogenation at 180, 200, and 250 °C. (b) Time dependence of the magnetization, M(t), normalized to its maximum initial value, M0, measured at 5 K after field cooling in magnetic field of 5 Oe, parallel to the c-axis, for the crystals hydrogenated at 180, 200, and 250 oC.

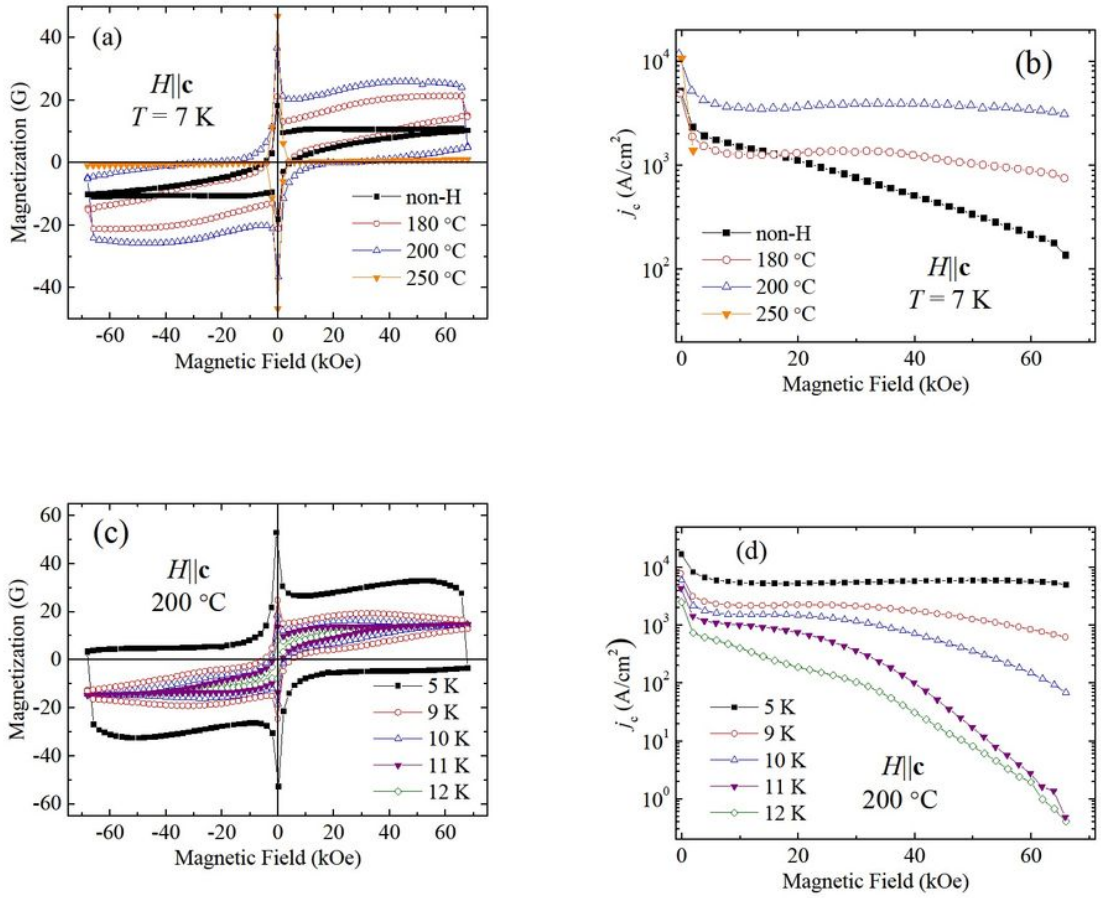

Figure 3

(a) Magnetization hysteresis loops recorded at 7 K for pristine FeTe0.65Se0.35 crystal and for the crystals hydrogenated at 180, 200, and 250 oC. (b) Field dependence of critical current density, jc, at 7 K for FeTe0.65Se0.35 single crystal: pristine and hydrogenated at 180, 200, and 250 oC. (c) Hysteresis loops recorded in the temperature range from 5 to 12 K for the crystal hydrogenated at 200 oC. (d) Comparison of field dependence of jc, recorded at various temperatures in the temperature range from 5 to 12 K, for the crystal hydrogenated at 200 oC.

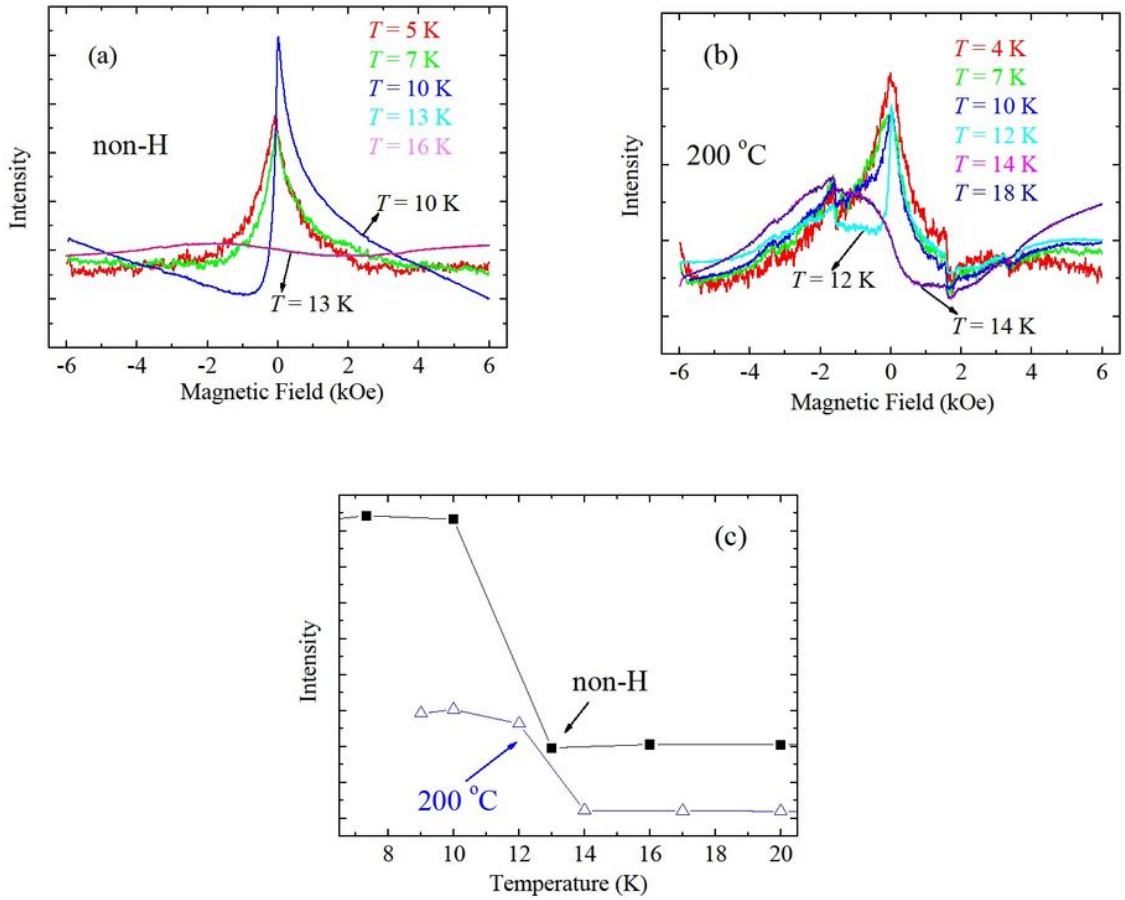

Figure 4

(a, b) Wide asymmetric lines observed in the temperature range of 4–18 K, which change significantly with decreasing temperature from 13 to 10 K (a), and from 14 to 12 K for the crystal hydrogenated at 200 oC (b). (c) Temperature dependence of the integrated intensity of the absorption line in the region close to bulk superconducting transition at about 13 K for both: as-grown and hydrogenated at 200 oC single crystals of FeTe0.65Se0.35.